Journal of Theoretical Biology 318 (2013) 129–139

Contents lists available at SciVerse ScienceDirect

Journal of Theoretical Biology

journal homepage: www.elsevier.com/locate/yjtbi

A metapopulation model for chikungunya including populations mobility on a large-scale network

Djamila Moulay [a,*], Yoann Pigné [b]

[a] LMAH, Normandy University, Le Havre, France
[b] LITIS, Normandy University, Le Havre, France

HIGHLIGHTS

- Study the effect of populations' mobility on a vector-borne disease.
- Focus on the chikungunya epidemic occurred in 2005–2006 on the Réunion Island.
- Proposition of a metapopulation model with a high-resolution patch network.
- Results show various consequences of the mobility on the disease spread.
- The model is validated against real epidemic data from the Réunion event.

ARTICLE INFO

Article history:
Received 21 February 2012
Received in revised form
28 October 2012
Accepted 3 November 2012
Available online 12 November 2012

Keywords:
Complex networks
Epidemiological models
Human mobility models
Metapopulation

ABSTRACT

In this paper we study the influence of populations mobility on the spread of a vector-borne disease. We focus on the chikungunya epidemic event that occurred in 2005–2006 on the Réunion Island, Indian Ocean, France, and validate our models with real epidemic data from the event. We propose a metapopulation model to represent both a high-resolution patch model of the island with realistic population densities and also mobility models for humans (based on real-motion data) and mosquitoes. In this metapopulation network, two models are coupled: one for the dynamics of the mosquito population and one for the transmission of the disease. A high-resolution numerical model is created from real geographical, demographical and mobility data. The Island is modeled with an 18,000-nodes metapopulation network. Numerical results show the impact of the geographical environment and populations' mobility on the spread of the disease. The model is finally validated against real epidemic data from the Réunion event.

1. Introduction

Many factors have influenced the emergence and re-emergence of vector-borne diseases (Gratz, 1999; Sutherst, 2004). Brutal changes in natural habitats such as massive or recurrent population migrations tend to speed up the spread of vector-borne diseases. The spatiotemporal evolution of such diseases is becoming a key issue for epidemiologists. To this purpose, models that consider the spatial distribution of a natural environment are of great interest. In this paper we are interested in the spatial spread of a vector-borne disease under the effect of human and vector mobilities. Indeed, human migration is one of the factors that have influenced the re-emergence of several diseases (Knobler et al., 2006; Martens and Hall, 2000). The modeling of geographical environments and population mobilities is becoming mandatory in this context. There are several approaches to describe such spread. One of the typical approaches, introducing spatial spread variation in epidemic models, involves the use of partial differential (Bailey, 1980; Murray, 2002; Fitzgibbon and Langlais, 2003). However, in the case of human mobility these approaches may not be appropriate. The theory of "metapopulation", first introduced in 1969 (Levins, 1969), in the field of ecology, allows such modeling. Several researches have been devoted to the study of disease spread in heterogeneous environments (Dushoff and Levin, 1995; Wang and Zhao, 2004; Lloyd and May, 1996). In Colizza and Vespignani (2008) and Cosner et al. (2009), authors study the influence of human dispersal among n patches in the dynamics of disease spread. In Balcan et al. (2010), authors, to study the spread of seasonal influenza, focus on air displacements and model the environment with a network where nodes are airports and edges represent flights. In Longini (1988) and Rvachev and Longini (1985), authors are also interested in the case of influenza and mobility in terms of long journeys. In Arino and Van den Driessche (2003), Arino (2009) and Arino et al. (2005), the authors propose a virus spread model based on this theory. In Menach et al. (2005) and Smith et al. (2004), the mobility of

* Corresponding author. Tel.: +33603385268.
E-mail addresses: djamila.moulay@univ-lehavre.fr, djamila.moulay@gmail.com (D. Moulay), yoann.pigne@univ-lehavre.fr (Y. Pigné).
URLS: http://djamila-moulay.org (D. Moulay), http://pigne.org (Y. Pigné).

0022-5193/$ - see front matter © 2012 Elsevier Ltd. All rights reserved.
http://dx.doi.org/10.1016/j.jtbi.2012.11.008

mosquitoes has been modeled to study the spatiotemporal dynamics of malaria. Other studies focus on direct-transmission diseases like Arino et al. (2005) and Arino and Van den Driessche (2003). In Balcan et al. (2010), influenza in the case of long trips (aircraft flights) is tackled. In Auger et al. (2008), the authors rely on the Ross–Macdonald model (Ross, 1910; Hackett, 1958), to consider human mobility.

Human mobility is usually considered in epidemic problems. Also, models that consider the dynamics of the vector population are numerous. However, to our knowledge, no model considers the coupling of population dynamics with populations mobility as we propose here. Moreover our approach promotes the consideration of vectors's mobility since the resolution of our model is greater than that of usual models.

In this paper we are proposing to couple two models (published in Moulay et al., 2010): a mosquito dynamics model (growth and evolution of the population) with a transmission virus model between two populations (humans and mosquitoes). The dynamics of the mosquito population is described by a stage structured model based on its biological life cycle. The different compartment states are egg, larva, pupa and adult. The disease transmission model is, for the human population, a SIR (Susceptible, Infected, Recovered) model. For adult mosquitoes, the transmission model is a SI (Susceptible, Infected) model.

Those two models are formalized using the metapopulation theory. It considers a network where nodes represent real habitats of the environment. In each of these nodes, transmission and population dynamics models appear and are coupled with neighbor nodes. Links in the network represent both the local neighborhood of a node and farther nodes that code for the mobility of humans.

We focus on a real case of chikungunya epidemic with the 2005–2006 event that occurred on the Réunion Island, a French island in the Indian Ocean. The island is modeled with a network. Since we want that network to reflect the local population's density, we consider the road network of the island as a proxy to the human density, considering that each crossroad is a node of the network. Then the local population on each node is adjusted according to real data given by the French Institute for Statistics (INSEE). Finally the entire island is modeled with an 18,000 nodes network.

In Gonzalez et al. (2008), authors propose various distributions that match a data set of real human mobility patterns (cell phone probes). We rely on these distributions to create human mobility patterns for the population in our model. We assume that individuals only change disease status when they are on a node and not during displacements. See Cui et al. (2006) for a model with disease transmission during travel.

Results show the decisive influence of mobilities over the spread of the disease. It is not only human mobility but also local vector interaction that plays an important role at the considered scale. Results are then compared to real epidemic data regarding the 2005–2006 event at the scale of the entire Réunion Island and the model is validated.

The remainder of this paper is organized as follows. The next section recalls original transmission and population dynamics models that this work is inspired from. Section 3 introduces the original metapopulation model that is able to include the previous models in a network of patches, linked to represent populations mobility. Then, in Section 4, according to the wish to validate the model against a real epidemic, a numerical implementation of the metapopulation model is constructed. This section details the construction of the metapopulation network in terms of environment and populations mobility. Section 5 presents various analyses performed on the model, showing the impact of mobilities. A validation is then proposed with a comparison with real epidemic data. Then a stochastic analysis of the model is proposed to study the robustness of the system. Finally Section 6 concludes the paper.

2. Original model

We first recall the model proposed and studied in Moulay et al. (2010) describing the vector dynamics. The formulated model is a stage structured model based on the biological mosquito life cycle. The vector population is subdivided into several classes: the aquatic stages consisting in eggs E and larvae/pupae L, and then the adult stage A, representing adult females. We assume first that the number of eggs b, laid by females, is proportional to the number of females itself. Second, the number of eggs and larvae are regulated by the effect of a carrying capacity K_E and K_L, respectively. Then we formulate a transmission virus model where the adult female stage A is subdivided into two epidemiological states: susceptible S_m and infectious I_m. It assumes that there is no vertical transmission of the virus, so that births from susceptible and infectious mosquitos occur in the egg stage with the same rate.

The human population consists in three epidemiological states: susceptible (or non-immune) S_H, infectious I_H, and removed (or immune) R_H. It is assumed that there is no vertical transmission of the disease, so that all births occur in the susceptible human class, at the rate $b_H > 0$. Moreover, we assume that the total human population N_H remains constant, and thus birth and death rates are equal. An infected human is infectious during $1/\gamma_h$ days, called the viremic period, and then becomes resistant or immune.

Forces of infections used in the model, which describe the rates of apparition of new infections, are standard and modeled by the mass–action principle normalized by the total population of humans, given by $\beta_m I_H(t)S_m(t)/N_H$ and $\beta_H I_m(t)S_H(t)/N_H$ where β_m and β_H are the transmission parameters.

These hypothesis are summed up in Fig. 1.

Based on our model description (see Fig. 1) and assumptions, we establish the following equations:

$$\begin{cases} \dfrac{dE}{dt}(t) = bA(t)\left(1-\dfrac{E(t)}{K_E}\right)-(s+d)E(t) \\ \dfrac{dL}{dt}(t) = sE(t)\left(1-\dfrac{L(t)}{K_L}\right)-(s_L+d_L)L(t) \\ \dfrac{dA}{dt}(t) = s_L L(t)-d_m A(t) \\ \dfrac{dS_m}{dt}(t) = s_L L(t)-d_m S_m(t)-\beta_m \dfrac{I_H(t)}{N_H} S_m(t) \\ \dfrac{dI_m}{dt}(t) = \beta_m \dfrac{I_H(t)}{N_H} S_m(t)-d_m I_m(t) \\ \dfrac{dS_H}{dt}(t) = -\beta_H \dfrac{I_m(t)}{N_H} S_H(t)+b_H(S_H(t)+I_H(t)+R_H(t))-d_H S_H(t) \\ \dfrac{dI_H(t)}{dt} = \beta_H \dfrac{I_m(t)}{N_H} S_H(t)-\gamma I_H(t)-d_H I_H(t) \\ \dfrac{dR_H(t)}{dt} = \gamma I_H(t)-d_H R_H(t) \end{cases} \tag{1}$$

The study of the model is detailed in Moulay et al. (2010). For this model (1), the second basic reproduction number is given by

$$R_0 = \frac{\beta_m \beta_H}{d_m(\gamma+b_H)} \frac{1}{N_H} \left(1-\frac{1}{r}\right) \frac{sK_E s_L K_L}{d_m(sK_E+(s_L+d_L)K_L)}$$

where $r = (b/(s+d))(s/(s_L+d_L))(s_L/d_m)$.

The threshold r governs the dynamics of mosquitoes. In this paper we assume that $r > 1$. This ensures the existence, persistence and global stability of a unique endemic equilibrium (E^*, L^*, A^*), which corresponds to the biological and interesting

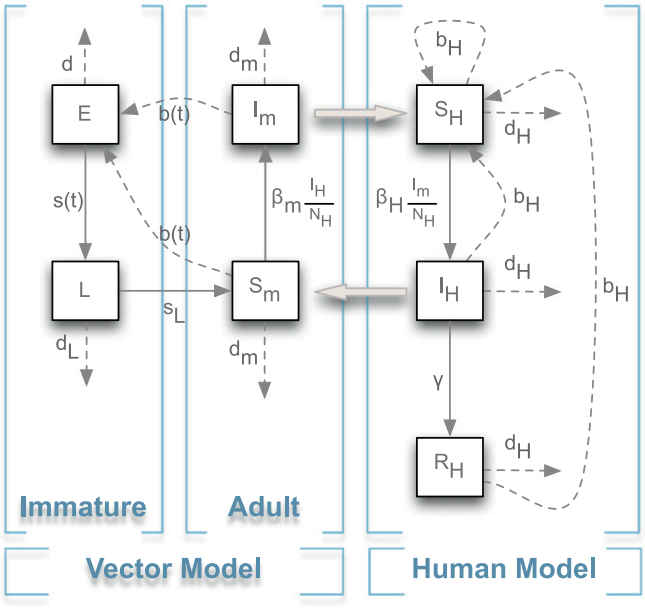

Fig. 1. Compartmental model for the dynamics of *Aedes albopictus mosquitos* and the virus transmission to human population. $b(t)=bA(t)(1-E(t)/K_E)$, $s(t)=sE(t)(1-L(t)/K_L)$ and the parameters of the model are given in Table 1.

case. The second reproduction number R_0 governs the dynamics of the transmission model.

3. Metapopulation model

In Arino (2009), Arino et al. (2005) and Arino and Van den Driessche (2003), Arino et al. formulate a general system of differential equations allowing to describe human mobility. In this model, they identify each population by its origin and its present location. We rely on this model and extend it with the definition of a neighborhood in which humans and mosquitoes interact.

3.1. Human mobility

Based on the model given in Arino (2009), Arino et al. (2005) and Arino and Van den Driessche (2003), we proposed an extension of our previous model (Moulay et al., 2010) to describe the spread of chikungunya under human and vector mobilities on a large-scale network.

Assume that the number of nodes in the network is n. A human population is identified due to two characteristics: the node from which he is originated, *i.e.* his residence and the node where he is at time t. We assume that the total human population is constant, *i.e.* births and deaths occur with the same rate $b_H=d_H$. Moreover, we suppose that births occur in the resident node while deaths take place in any node where the human is present.

Let us denote by $S_{Hij}(t)$, $I_{Hij}(t)$ and $R_{Hij}(t)$ respectively the susceptible, infected and removed human populations originated from node i and present on node j at time t. We denote by S_{mi} and I_{Hi} the susceptible and infected mosquitoes present in node i respectively. In the first assumption mosquitoes mobility is neglected, which looks realistic compared to the distance of human displacements. So, resident mosquitoes from node i are also present on this node.

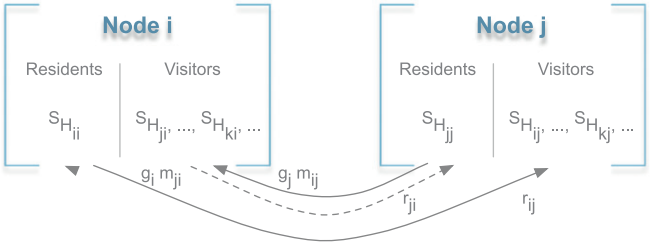

Fig. 2. Human population mobility between nodes i and j.

The total number of susceptible, infected and removed human residents of node i is given, respectively, by $S_{H_i}^r=\sum_{j=1}^n S_{Hij}$, $I_{H_i}^r=\sum_{j=1}^n I_{Hij}$ and $R_{H_i}^r=\sum_{j=1}^n R_{Hij}$. The total number of susceptible, infected and removed human present on node i is given, respectively, by $S_{H_i}^p=\sum_{j=1}^n S_{Hji}$, $I_{H_i}^p=\sum_{j=1}^n I_{Hji}$ and $R_{H_i}^p=\sum_{j=1}^n R_{Hji}$. The number of human residents on node i is then equal to $N_{H_i}^r=S_{H_i}^r+I_{H_i}^r+R_{H_i}^r$ and the human population present on node i is $N_{H_i}^p=S_{H_i}^p+I_{H_i}^p+R_{H_i}^p$.

As in Sattenspiel and Simon (1988) and Arino and Van den Driessche (2003), we define the travel rate from node i to node j by $g_i m_{ji}$, where $g_i\geq 0$ corresponds to the per capita rate at which residents of node i leave this node and a fraction $m_{ji}\geq 0$ of them go to node j, with $m_{ii}=0$. Residents of node i, present on node j, then return to node i with a per capita rate $r_{ij}\geq 0$, with $r_{ii}=0$. Displacements between two nodes are represented in Fig. 2.

The dynamics of human populations (susceptible, infected and removed) resident and present on node i is given by

$$\frac{dS_{Hii}}{dt}=d_H(N_{H_i}^r-S_{Hii})-g_iS_{Hii}+\sum_{k=1}^n r_{ik}S_{Hik}-\beta_{Hi}\frac{Im_i}{N_{H_i}^p}S_{Hii}$$

$$\frac{dI_{Hii}}{dt}=-d_HI_{Hii}-g_iI_{Hii}+\sum_{k=1}^n r_{ik}I_{Hik}+\beta_{Hi}\frac{Im_i}{N_{H_i}^p}S_{Hii}-\gamma_HI_{Hii}$$

$$\frac{dR_{Hii}}{dt}=-d_HR_{Hii}+\gamma_HI_{Hii}-g_iR_{Hii}+\sum_{k=1}^n r_{ik}R_{Hik}$$

The dynamics of human populations (susceptible, infected and removed) resident on node i and present on node j is given by

$$\frac{dS_{Hij}}{dt}=-d_HS_{Hij}+g_im_{ji}S_{Hii}-r_{ij}S_{Hij}-\beta_{Hj}\frac{Im_j}{N_{H_j}^p}S_{Hij}$$

$$\frac{dI_{Hij}}{dt}=-d_HI_{Hij}+g_im_{ji}I_{Hii}-r_{ij}I_{Hij}+\beta_{Hj}\frac{Im_j}{N_{H_j}^p}S_{Hij}-\gamma_HI_{Hij}$$

$$\frac{dR_{Hij}}{dt}=-d_HR_{Hij}+g_im_{ji}R_{Hii}-r_{ij}R_{Hij}+\gamma_HI_{Hij}$$

The dynamics of mosquito populations (eggs, larvae and pupae, adult females) given in Moulay et al. (2010) in each node is

$$\frac{dS_{mi}}{dt}=s_LL_i-d_mS_{mi}-\beta_{mi}\frac{S_{mi}}{N_{H_i}^p}I_{H_i}^p \tag{2a}$$

$$\frac{dI_{mi}}{dt}=\beta_{mi}\frac{S_{mi}}{N_{H_i}^p}I_{H_i}^p-d_mI_{mi} \tag{2b}$$

$$\frac{dE_i}{dt}=b(S_{mi}(t)+I_{mi}(t))\left(1-\frac{E_i(t)}{K_{Ei}}\right)-(s+d)E_i(t) \tag{2c}$$

$$\frac{dL_i}{dt}=sE_i(t)\left(1-\frac{L_i(t)}{K_{Li}}\right)-(s_L+d_L)L_i(t) \tag{2d}$$

where the dynamic of immature stages E and L is described by corresponding equations in system (1).

Remark 1.

(i) Note that the infection transmitted in node i between susceptible mosquitoes and infected humans depends now on the human population present on this node $N_{H_i}^p$
$\sum_{j=1}^{n} \beta_{mi}\frac{S_{mi}}{N_{H_i}^p} I_{Hji} = \beta_{mi}\frac{S_{mi}}{N_{H_i}^p} I_{H_i}^p$

(ii) The distance between nodes is not explicitly taken into account; nevertheless it is implicitly included in the coefficients m_{ji} and r_{ij}.

(iii) In the following we focus on daily displacements; humans who leave their resident node, obviously return to their resident node on a daily basis. Displacement matrices $M^T=[g_i m_{ji}]$ and $R=[r_{ij}]$ have the same zero/nonzero pattern.

The human mobility model and the virus transmission dynamics are given by the following equation:

$$\frac{dS_{Hii}}{dt} = d_H(N_{H_i}^r - S_{Hii}) - g_i S_{Hii} + \sum_{k=1}^{n} r_{ik} S_{Hik} - \beta_{Hi}\frac{Im_i}{N_{H_i}^p} S_{Hii} \tag{3a}$$

$$\frac{dS_{Hij}}{dt} = g_i m_{ji} S_{Hii} - d_H S_{Hij} - r_{ij} S_{Hij} - \beta_{Hj}\frac{Im_j}{N_{H_j}^p} S_{Hij} \tag{3b}$$

$$\frac{dI_{Hii}}{dt} = -d_H I_{Hii} - g_i I_{Hii} + \sum_{k=1}^{n} r_{ik} I_{Hik} + \beta_{Hi}\frac{Im_i}{N_{H_i}^p} S_{Hii} - \gamma_H I_{Hii} \tag{3c}$$

$$\frac{dI_{Hij}}{dt} = g_i m_{ji} I_{Hii} - d_H I_{Hij} - r_{ij} I_{Hij} + \beta_{Hj}\frac{Im_j}{N_{H_j}^p} S_{Hij} - \gamma_H I_{Hij} \tag{3d}$$

$$\frac{dR_{Hii}}{dt} = \gamma_H I_{Hii} - d_H R_{Hii} - g_i R_{Hii} + \sum_{k=1}^{n} r_{ik} R_{Hik} \tag{3e}$$

$$\frac{dR_{Hij}}{dt} = g_i m_{ji} R_{Hii} + \gamma_H I_{Hij} - d_H R_{Hij} - r_{ij} R_{Hij} \tag{3f}$$

$$\frac{dS_{mi}}{dt} = s_L L_i^* - d_m S_{mi} - \sum_{j=1}^{n} \beta_{mi}\frac{S_{mi} I_{Hji}}{N_{H_i}^p} \tag{3g}$$

$$\frac{dI_{mi}}{dt} = \sum_{j=1}^{n} \beta_{mi}\frac{S_{mi} I_{Hji}}{N_{H_i}^p} - d_m I_{mi} \tag{3h}$$

where $L_i^* = (1-1/r)(K_{Li}/\gamma_{Li})$ and $\gamma_{Li} = 1+(((s_L+d_L)K_{Li})/sK_{Ei})$ are given by the endemic equilibrium of the vector population dynamic model. In this model, each node is described by $(3n+2)n$ equations.

3.1.1. Equilibrium of the model

Proposition 3.1. *The nonnegative orthant $\mathbb{R}_+^{(3n+2)n}$ is positively invariant under the flow of (3) and, for all $t>0$, $S_{Hii}>0$ and $S_{Hij}>0$ provided that $g_i m_{ji}>0$. Moreover, solutions of (3) are bounded.*

Proof. We easily see that solutions of system (3) remain non-negative. Indeed, it is sufficient to show that for all non-negative initial conditions, the vector-field points to the interior of the positive orthant. Assume now that $S_{Hii}=0$ at $t=0$, then $dS_{Hii}/dt = d_H N_{H_i}^r + \sum_{k=1}^{n} r_{ik} S_{Hik} > 0$, thus $S_{Hii}>0$ for $t>0$. Equally, if $S_{Hij}=0$ at time $t=0$, then $dS_{Hij}/dt = g_i m_{ji} S_{Hii} > 0$.

Finally, the boundedness follows from the positive invariance of $\mathbb{R}_+^{(3n+2)n}$ and the constant population property. Indeed $dN_{H_i}^r/dt = 0$, which means that, for any node i, the resident population is constant, and thus by extension, the whole population is constant. Moreover, solutions of (3) are bounded; since $(\mathbb{R}^+)^{(3n+2)n}$ is invariant, human population is constant and vector population is bounded (Moulay et al., 2010). □

Definition 3.2 (*Arino, 2009*). 1. The system is at equilibrium if the time derivatives in (3) are zero.

2. A node i is at the disease free equilibrium (DFE) if $I_{Hji}=0$, $I_{mi}=0$ for all $j=1,\ldots,n$.

3. The n-nodes model given by (3) is at the DFE if each node is at the DFE, *i.e.*, $I_{Hji}=0$ and $I_{mi}=0$, for all $i,j=1,\ldots,n$.

Proposition 3.3. *System (3) always has the following disease free equilibrium*:

$$S_{Hii}^* = \left(\frac{1}{1+g_i\sum_{k=1}^{n}\frac{m_{ki}}{d_H+r_{ik}}}\right) N_{H_i}^r, \quad S_{Hij}^* = g_i\frac{m_{ji}}{d_H+r_{ij}} S_{Hii}^*$$

$$I_{Hii}^* = 0, \quad I_{Hji}^* = 0$$

$$R_{Hii}^* = 0, \quad R_{Hji}^* = 0$$

$$S_{mi}^* = \frac{s_L}{d_m} L_i^*, \quad I_{mi}^* = 0, \quad \text{for all } i,j=1,\ldots,n,\ i\neq j.$$

Proof. It is sufficient to remark that

$$1 - \sum_{k=1}^{n}\frac{m_{ki} r_{ik}}{d_H+r_{ik}} = \sum_{k=1}^{n} m_{ki} - \sum_{k=1}^{n}\frac{m_{ki} r_{ik}}{d_H+r_{ik}} = d_H\sum_{k=1}^{n}\frac{m_{ki}}{d_h+r_{ik}}. \qquad \square$$

Theorem 3.4 (*Arino, 2009*). *Assume that system (3) is at equilibrium and a node i is at the DFE. Then all nodes that can be accessed from node i and all nodes that have an access to node i are at the DFE. Moreover, if the outgoing matrix M^T is irreducible, then all nodes are at the DFE.*

Proof. See appendix.

Definition 3.5 (*Arino, 2009*). The disease is endemic within the population if the number of infective individuals is positive in this population.

The disease is endemic on node i if there is a population on node i in which the disease is endemic, *i.e.*, there exists $k\in\{1,\ldots,n\}$ such as $I_{Hki}>0$.

Theorem 3.6 (*Arino, 2009*). *Assume that system (3) is at equilibrium and the disease is endemic on node i. Then the disease is endemic on all nodes that can be reached from node i. In particular, if the matrix M^T is irreducible, then the disease is endemic in all nodes.*

Proof. See appendix.

3.2. The vector mobility model

Contrary to human displacements, it is unrealistic to identify mosquitoes by their origin and destination. Nevertheless, we know that *Aedes albopictus* mosquitoes have a limited flight range. Most mosquitoes disperse less than 200 m away from their original breeding place (Vermillard, 2009; Nishida and Tenorio, 1993). Indeed, mosquitoes present in a node i may have activity in neighboring nodes j, depending on their proximity (defined later). Metapopulation models of the spread of vector-borne diseases (see for instance Zongo, 2008; Tsanou, 2011) that include human long-distance displacements do not take into account mosquito mobility. In our case of daily movements and very precise resolution, we cannot neglect the influence of mosquito displacements. We propose to model this activity using the biological radius of interaction around their breeding sites. Let us denote by d_{ij} the distance between nodes i and j and by d_{max} the maximum

interaction radius of mosquitoes (approximately 200 m). In particular, we have $d_{ii}=0$ for all $i=1,\ldots,n$. Now we assume that mosquitoes originated from node i interact with the population of node j, according to a function of the distance linearly decreasing. This function is given by

$$\psi(d_{ij})=\begin{cases}\dfrac{d_{max}-d_{ij}}{d_{max}} & \text{if } d_{ij}<d_{max}\\ 0 & \text{else}\end{cases} \tag{4}$$

Then, model (3) becomes

$$\frac{dS_{Hii}}{dt}=d_H(N_{H_i}^r-S_{Hii})-g_iS_{Hii}+\sum_{k=1}^{n}r_{ik}S_{Hik}-\sum_{k=1}^{n}\beta_{Hi}\psi(d_{ik})\frac{Im_k}{N_{H_i}^p}S_{Hii} \tag{5a}$$

$$\frac{dS_{Hij}}{dt}=g_im_{ji}S_{Hii}-d_HS_{Hij}-r_{ij}S_{Hij}-\sum_{k=1}^{n}\beta_{Hj}\psi(d_{ik})\frac{Im_k}{N_{H_j}^p}S_{Hij} \tag{5b}$$

$$\frac{dI_{Hii}}{dt}=-d_HI_{Hii}-g_iI_{Hii}+\sum_{k=1}^{n}r_{ik}I_{Hik}+\sum_{k=1}^{n}\beta_{Hi}\psi(d_{ik})\frac{Im_k}{N_{H_i}^p}S_{Hii}-\gamma_HI_{Hii} \tag{5c}$$

$$\frac{dI_{Hij}}{dt}=g_im_{ji}I_{Hii}-d_HI_{Hij}-r_{ij}I_{Hij}+\sum_{k=1}^{n}\beta_{Hj}\psi(d_{ik})\frac{Im_k}{N_{H_j}^p}S_{Hij}-\gamma_HI_{Hij} \tag{5d}$$

$$\frac{dR_{Hii}}{dt}=\gamma_HI_{Hii}-d_HR_{Hii}-g_iR_{Hii}+\sum_{k=1}^{n}r_{ik}R_{Hik} \tag{5e}$$

$$\frac{dR_{Hij}}{dt}=g_im_{ji}R_{Hii}+\gamma_HI_{Hij}-d_HR_{Hij}-r_{ij}R_{Hij} \tag{5f}$$

$$\frac{dS_{mi}}{dt}=s_LL_i-d_mS_{mi}-\sum_{k=1}^{n}\beta_{mi}\psi(d_{ik})\frac{S_{mi}}{N_{H_k}^p}I_{H_k}^p \tag{5g}$$

$$\frac{dI_{mi}}{dt}=\sum_{k=1}^{n}\beta_{mi}\psi(d_{ik})\frac{S_{mi}}{N_{H_k}^p}I_{H_k}^p-d_mI_{mi} \tag{5h}$$

which describes both the vector population dynamic and the virus transmission, through the human and vector mobilities in the network. Note that aquatic stages of eggs and larvae remain described by Eq. 2(c) and (d) and complete the model.

4. Application

Willing to validate this approach, this section proposes a comparison of this model with a real-life example of chikungunya epidemic, namely the event that occurred in 2005–2006 on the Réunion Island, Indian Ocean. This validation process makes a strong usage of real and realistic data to reflect the original environment as much as possible. This last one is modeled based on real geographical information. Populations mobility is modeled following existing real data analysis. Finally, epidemiological results are compared to real data from the 2005–2006 event.

4.1. Distribution of the human population

The Réunion Island is a mountainous region and the local population is not uniformly spread over the land. To reflect this particular density in the metapopulation model, we rely on two realistic sources of information.

The INSEE gives access to an estimated density of the population, based on a mesh zoning of the space (INSEE, 2012). This zoning consists of squares of one kilometer length. In each square, the number of people living is estimated based on both tax cards and cadastral data. Fig. 3 shows these 1 km^2 squares with their associated population.

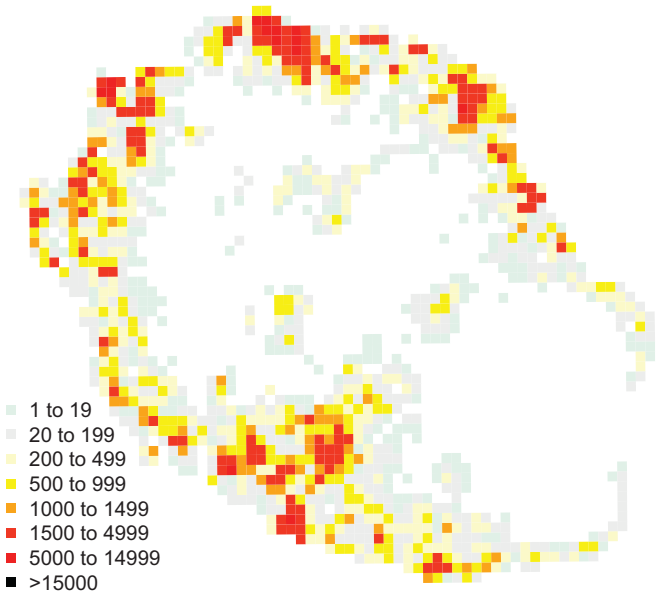

Fig. 3. Estimated population distribution of the Réunion in 2007, according to the French Institution for Statistics, on a 1 km^2 granularity.

There is good confidence in the quality of this data; however, the limited granularity of one square kilometer is not precise enough for our purpose. Indeed this model envisions a lower scale of interaction between humans and mosquitoes, since the latter only have a couple hundreds of meters interaction range.

Second, the road network is used as a proxy to the human density. Indeed, the road network is denser where the population is itself dense, and lighter where no one lives. Data extracted from OpenStreetMap (OSM) (OpenStreetMap, 2012) provide road information and especially road intersections at a high resolution (scale of one meter). We propose to use those intersections as the nodes of the metapopulation model.

Then the human population is distributed on these nodes. Each of them belongs to one of the 1 km^2-areas of the INSEE. So, on each of these squares, the local population can be evenly distributed among its own nodes. If a square has no node associated to it (it happens on low density areas) then a single node is created with the corresponding population.

Finally, this distribution is at least as relevant as the real data given by the INSEE at the scale of 1 km^2, but the resolution goes below the 1 km limit, thanks to the crossroad/node analogy. Fig. 4 illustrates the main steps of the construction of the model.

4.1.1. Distribution of the mosquito population

No information about the density of mosquito population is available. Moreover, we are not interested in the whole population but rather in the part of it that interacts with humans. Our hypothesis is that the density of mosquitoes is homogeneous.

To retrieve this density from the human-centered network, each node is given a number of mosquitoes (through the carrying capacities) proportional to the geographical surface associated with that node, thanks to a simple Voronoï tessellation.

Since we only consider mosquitoes that interact with humans, the surface is upper-bounded with the disk of radius d_{max} that expresses the maximum interaction distance for a mosquito in its life.

Let S_i be the surface of node i. Let $S_{max}=\pi d_{max}^2$ be the surface associated with the maximal interaction radius d_{max}. Carrying

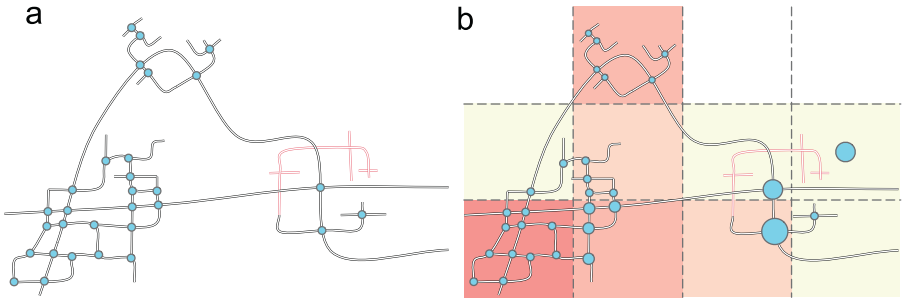

Fig. 4. Schematic construction of the nodes of the metapopulation network. (a) Network nodes are the road intersections, knowing that this network may not be totally accurate (red roads missing in the map). (b) Distribution of the population on nodes according to the INSEE data. Empty cells (with no known road network) are given one node (as in (b), second row, rightmost cell). (For interpretation of the references to color in this figure legend, the reader is referred to the web version of this article.)

capacities for each node are then set as follows: $K_{E_i} = K_E\ \varphi(S_i)$ and $K_{L_i} = K_L\ \varphi(S_i)$, with K_E and K_L, constants for the carrying capacities of eggs and larvae, respectively, and $\varphi(S_i)$ is equal to S_i/S_{max} and is upper bounded by 1.

4.1.2. Human mobility

In the model, human trips are given by outgoing matrix M^T and incoming matrix R and represent for any pair i and j, the probability for humans living on i to go to j. Non-null values in the matrix define edges between nodes in the metapopulation network.

To reach realistic motion we need to rely on realistic data or the model for human mobility. Unfortunately, we could not get such information for the Island, so we rely on some more general analysis work from M. C. González, C. A. Hidalgo and A. Barabási (Gonzalez et al., 2008) who analyzed mobile phone communication logs of 100,000 users. These logs register the geographical position of mobile phones when calls happen or when texts are emitted/received. Mobile phones are a good proxy for human mobility because users always carry their phone.

The authors were able to produce general laws on observed mobility patterns. These results give general formulas that describe the mobility observed. We use these formulas to generate new human mobility patterns. We consider the three following measures.

Trips length: The distribution of the length of a human trip Δr in kilometer according to the following power law:

$$P(\Delta r) = (\Delta r + \Delta r_0)^{-\beta} \exp(-\Delta r/\kappa) \tag{6}$$

where $\Delta r_0 = 1.5$ km is the cutoff value of the law and $\kappa = 80$ km.

Presence probability: Given N possible destinations for each individual, their presence probability in each destination is approximated with the following Zipf law:

$$f(k;N) = \frac{1/k}{\sum_{n=1}^{N}(1/n)}$$

where k is the rank of each destination when decreasingly sorted.

Return probability: The authors observe that there is a peak of probability of returning to the same place every 24 h. In other words, the human mobility mainly follows a daily pattern such as home/work trips.

From these measures we generate artificial per-individual trips on the island that respect the observed properties in the original data set.

Remark 2. The model defines matrices M^T and R as tables indicating respectively departures and returns. The mobility model we could create from Gonzalez et al. (2008) however gives the probability of presence for a human, given all its possible destinations. Our hypothesis here is that there is a link between departures/returns probabilities and presence probabilities that we do not investigate in this paper.

Table 1
Parameters of the mosquito and transmission dynamics models. Most of the values were obtained from other publications in the field (Bacaer, 2007; Delatte et al., 2009; Dumont and Chiroleu, 2010; Moulay et al., 2012).

Parameters	Description	Value
b	Oviposition rate	6.0
K_E	Egg carrying capacity	1000
K_L	Larva carrying capacity	$K_E/2$
s	Transfer rate $E \to L$	1/3
s_L	Transfer rate $L \to A$	1/10
d	Egg mortality rate	1/3
d_L	Larva mortality rate	1/3
d_m	Female adult mortality rate	1/14
b_H	Human birth/death rate	1/(78∗365)
β_H	Infection rate: vector to human	See Section 5.5
β_m	Infection rate: human to vector	See Section 5.5
γ_H	Human recovery rate	1/7

4.1.3. Mosquito mobility

As stated in the model description, mosquitoes are not identified with origins and destinations. Since we are aware of their limited flight range, their mobility is thus defined by a geographical disk area of interaction centered at their origin node. Function (4) defines their interaction with humans.

This new mobility pattern is constructed, in the metapopulation network, with edges linking nodes that are below the interaction range d_{max}.

5. Results

In this section we show and discuss results of the simulation of our metapopulation model applied to the scenario of the Réunion Island described in the previous section. Our results are then compared with real data from the 2005–2006 epidemic event.

5.1. Analysis of the metapopulation network

The metapopulation network can be represented by two graphs sharing the same set of nodes, or in other words, it is a graph with two subsets of edges. One subset is for human mobility and one is for mosquito mobility. The purpose of Table 2 is to give some metrics for those two graphs to give a general overview of their dimensions. Indeed due to its size visualization of all networks is not proposed since it does not give any useful information.

5.2. Spread of the disease in the network

In this scenario we observe the spread of the disease with one infected individual put on one node of the network. Provided infection parameters (β_H and β_m) are set high enough, the insertion of this individual in a system at disease-free equilibrium may start an epidemic event. Three nodes of the network are monitored: the first where the individual was inserted, a one-hop neighbor, and a farther one located 6 km from the insertion node. Four metrics are observed: susceptible humans (S_H), susceptible mosquitoes (S_m), infected humans (I_H), and infected mosquitoes (I_m).

Fig. 5 shows, as expected, a shift in time of the evolution from the closest nodes to the farther one. However, that shift (and thus the spread of the disease) is not proportional to the geographical distance between nodes but rather to a graph distance. The third observed node is 60 hops far from the insertion node in the mosquito mobility graph and only four hops away in the human mobility graph. Human mobility, thus, greatly speeds up the spread.

Table 2
Metrics for the two graphs of the metapopulation network.

Metric	Mosquitoes	Humans
Number of nodes	17,988	17,988
Number of links	151,772	744,313
Average degree	≈ 17	≈ 83
Connectivity	no (1729 connected components)	Yes
Diameter	71 (for the biggest component)	15

5.3. Consequences of the mosquito mobility

As stated in the Introduction, most of the metapopulation models on vector-borne viruses focus on long distance and long duration journeys for the human population. In those models the vector mobility can easily be ignored. Here we consider daily-based mobility with short journeys. We believe this shorter scale in time and space brings the new constraint that mosquito mobility cannot be neglected anymore.

The effect of local mosquito interaction is shown with a scenario where again, a disease free population is inserted with an infected human. Two experiments are carried out, one with mosquito mobility and one without. Human mobility is kept in both scenarios.

Fig. 6 shows the number of instantaneous infected humans (I_H). The infection starts rapidly and is concentrated with mosquito mobility enabled. Oppositely, without this mobility, the spread takes more time to start and the peak is less important. It is clear that mosquito mobility at this scale has to be considered.

5.4. Consequences of the human mobility

Human mobility has an obvious effect on the mobility. The purpose here is to analyze realistic and slight modifications of this mobility like quarantine measures that may be taken in case of epidemics.

This scenario proposes to stop the human mobility on infected parcels. So quarantine measures will be localized only on nodes where a given threshold of infection is reached. In quarantined nodes inhabitants are not allowed to move out and no foreigners

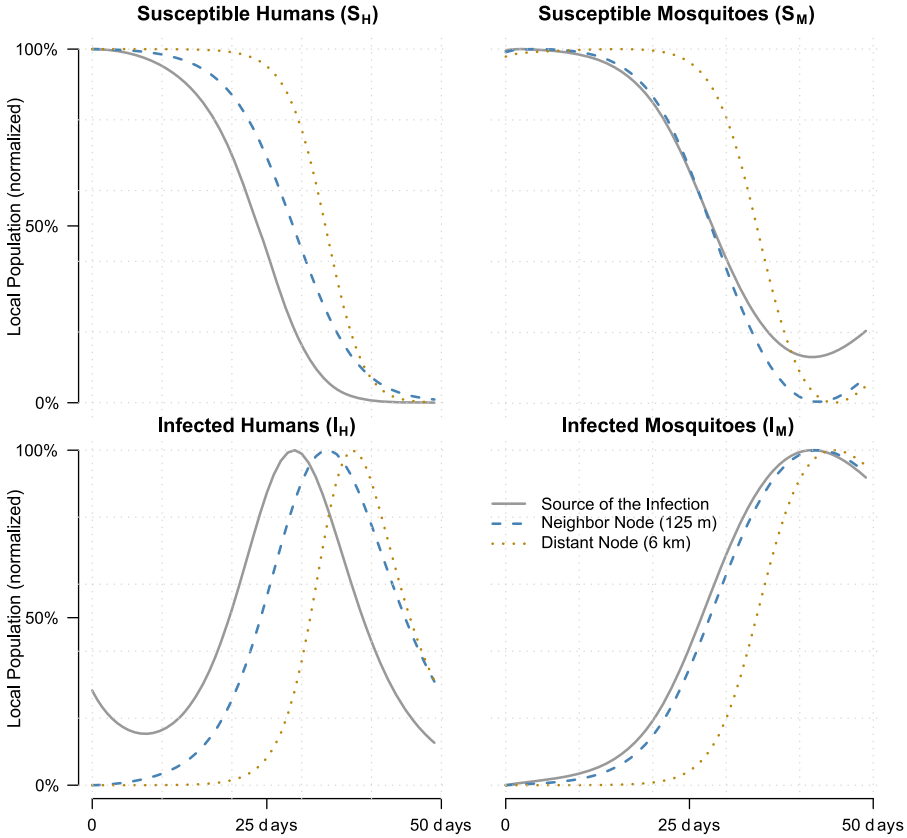

Fig. 5. Spread of the disease in the network for three observed nodes. The first is the infected human. The second is an immediate neighbor (125 m away from the first). The third, 6 km away from the first node, is 60 hops away in the mosquito mobility graph and 4 hops away in the human mobility graph. Quantities of population (y-axis) are normalized. A shift (or delay) effect in the spread is observed.

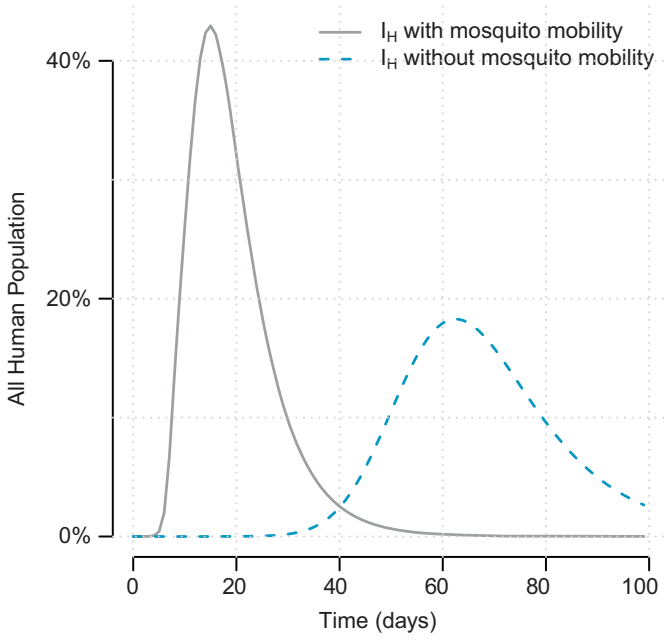

Fig. 6. Effect of mosquito mobility of the spread of an epidemic. Evolution of the number of infected humans (I_H) with and without mosquito mobility. In order to obtain comparable results, infection rates as set to a relatively high level: $\beta_H = 0.2$, $\beta_m = 0.15$.

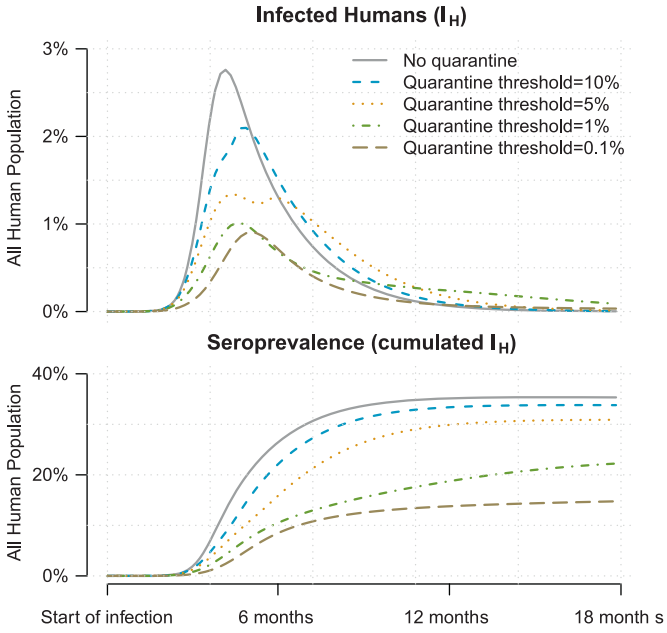

Fig. 7. Consequences of the human mobility. The instantaneous number of infected humans and the seroprevalence (or number of people ever infected) is observed during an epidemic. Infection values depend on the quarantine threshold that reduce, node per node, the human mobility, over the time. A threshold of 10% indicates that a node with an infection rate of at least 10% will be quarantined (incoming and outgoing human mobility are blocked).

are allowed in. Since mosquitoes are not stopped by quarantine measures, they continue to interact within all nodes.

Fig. 7 shows global instantaneous and cumulated infection values for humans at the scale of all populations. In this scenario, the disease would, without any control, reach 35% of the population, just like the chikungunya event of 2005–2006.

Results show the possibility to rapidly reduce the instantaneous infection rate. For instance, the I_H peak is almost divided by two when the quarantine threshold is set to 10%. However, looking at cumulated infection cases (seroprevalence), such a threshold does not significantly reduce the total amount of infections. To expect a real effect on the total number of infections one have to set the threshold below 1%. Here, each node on average has less than 50 humans, so any threshold below 2% is technically impossible to achieve.

5.5. Parameters analysis

The identification of predominant parameters of the system is needed to understand its behavior. We propose here a numerical analysis of the parameters of the system. An in depth statistical sensitivity analysis or the analytical estimation of parameters would be of great interest too, but are out of the scope of this paper.

Infection rate parameters, β_H (mosquitoes to humans) and β_m (humans to mosquitoes) have a strong impact on the results. Depending on the values selected for β_H and β_m, the infection goes from a few isolated cases to an epidemic that contaminates the whole population.

Fig. 8 shows a scatter plot of values taken by β_H and β_m. For each couple (β_H, β_m) the seroprevalence (after 400 days of epidemic) is observed. Values in percentage represent the ratio of the total human population ever infected depending on the two parameters. Contour lines help in finding, given a seroprevalence percentage, values for β_H and β_m. These values are used in the validation.

5.6. Validation against real data

We propose a validation with a comparison against real data from the 2005–2006 chikungunya epidemic. The two first cases of chikungunya where reported at the beginning of March 2005. The disease propagated during the following weeks and reached a peak at mid of May. The number of new cases then started to decrease until authorities thought the event was over at the end of the year 2005 with a seroprevalence (total number of cases) of

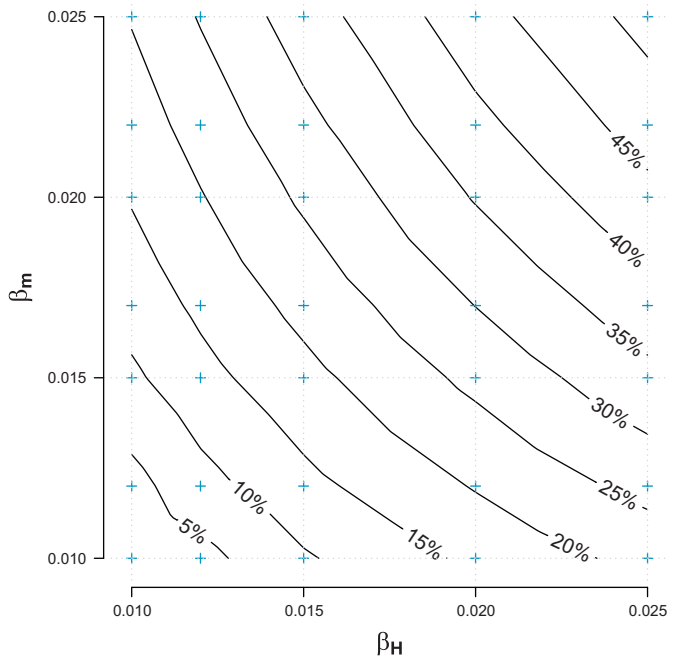

Fig. 8. Effect of β_H and β_m parameters on the seroprevalence. Blue crosses are values obtained by simulation. Contour lines are obtained with a bilinear interpolation of these data points. (For interpretation of the references to color in this figure legend, the reader is referred to the web version of this article.)

6,000 people. But in the second half of December 2005 the spread started over with a strength that was not comparable to the previous peak. This second event reached a peak in February 2006 with more than 47,000 cases in a week. This sudden reactivation of the spread was later explained by a genetic mutation of the virus that lead to a new and more infective strain (Vazeille et al., 2007). After the peak, the number of cases slowly started to decrease. The epidemic was declared over by April 2006. In the end, the InVS (French Institute for Health Care) counted 265,733 cases of chikungunya from March 2005 to April 2006. This represents more than 35% of the total population of the Island.

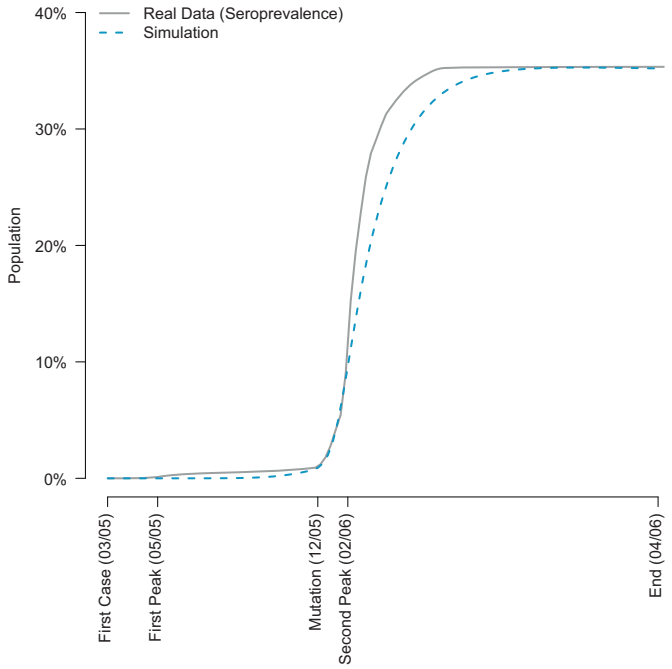

Fig. 9. Comparison of the model with real data. The seroprevalence is considered for the duration of the Réunion Island epidemic. Values of β_H and β_m are 0.0118 and 0.0101, before the mutation event and 0.0245 and 0.0161, after respectively. Those two couples (β_H,β_m) are chosen thanks to the study in Section 5.5. Values for the other parameters of the system are given in Table 1.

The following results are compared to real data indicating, week per week, new cases of the disease. This information was kindly provided by the InVS.

Back to our model, the new virus strain with its stronger infection rate is modeled thanks to infection rates β_H and β_m. We try to reproduce all the events by starting the simulation of the epidemic with one set of parameters, and then, by changing only one time the values of β_H and β_m at the moment it appears in the real event. The two sets of parameters were selected experimentally with the help of the previous study (see Fig. 8) giving possible values for β_H and β_m for a given seroprevalence.

Fig. 9 compares the evolution of the real seroprevalence of the chikungunya event, with simulation results obtained with our model. Although the two curves do not fit perfectly, it allows a visual overall validation of the model.

These results are a first step in the validation of this approach. In these experiments, only infection rates were investigated. Of course, other parameters need to be considered especially those leading the human mobility. Moreover, the metapopulation approach needs to be validated at a lower scale than the scale of the entire Island. These last observations form the perspectives of this work.

5.7. *Stochastic analysis of the model*

The model can be affected by stochastic changes. Indeed, the human mobility given by matrices M^T and R is defined according to the mobility probability law given in Gonzalez et al. (2008).

We propose to study the robustness of the system by running simulations of the model with various instances of the human mobility matrices and thus observe the variations in the obtained results. The population itself and the number of displacements do not change, only the destinations are different.

Fig. 10 illustrates the evolution of infected humans on various (randomly chosen) nodes in the network, within the very same scenario that the mutation experiment described in Section 5.6. We assume that observations made on I_H also apply on the other outputs of the model. Thirty different human mobility matrices are used. The figure shows that the height of the variation, although different on each node, remains within coherent

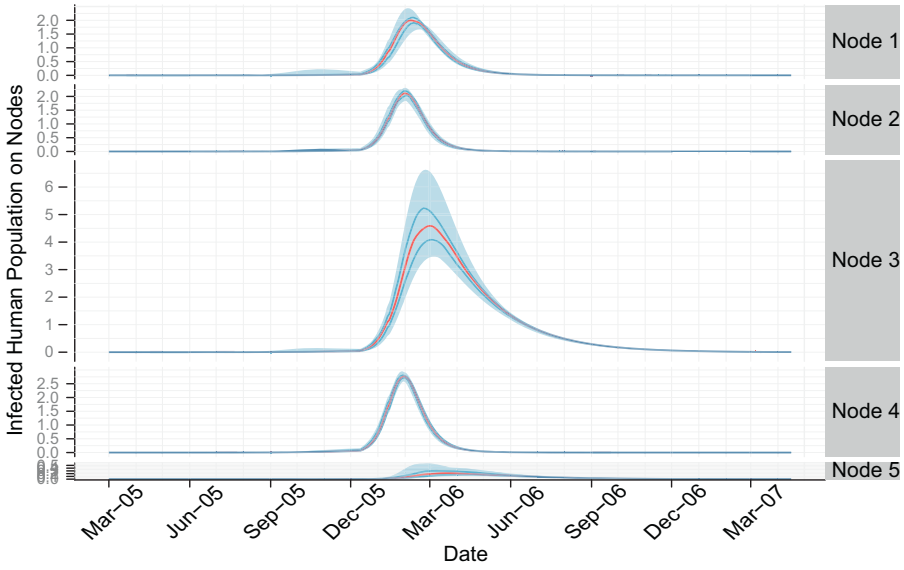

Fig. 10. Statistics on I_H for a random selection of nodes. The blue ribbon shows minimum and maximum values over the 30 experiments. Darker blue curves show first and third quartiles while the red curve shows the median. (For interpretation of the references to color in this figure legend, the reader is referred to the web version of this article.)

Table 3
Highest values of standard deviation (SD) for I_H on a random selection of nodes.

	Node 1	Node 2	Node 3	Node 4	Node 5
Population	24	16	932	21	78
SD	0.27	0.16	0.76	0.17	0.13
Date of SD (in 2006)	1–24	1–16	2–15	1–12	2–21
% of population	1.11	1.05	0.08	0.84	0.16

boundaries. Indeed when considering, for each node, the date when the standard deviation is the highest, compared to the node's population, it remains below 2% of that population, as illustrated in Table 3.

When considering simulation results at the scale of the whole network, the variation is even lower with a maximum standard deviation (on 10 January, 2016) of 544 infected humans which represents less that 0.07% of the population of the Island.

These results tend to confirm the robustness of the system against stochastic variations.

6. Conclusion

In this work the main concern was to try to validate dynamical systems for the spread of a vectorial disease against a real epidemic scenario. We focused on the Réunion Island epidemic that occurred in 2005–2006.

Many issues appear when trying to bridge the gap between global models and real life problems. Among them we chose to focus on the modeling of populations' mobilities. This logically implied a realistic modeling of environment, bringing us from temporal modeling to spatio-temporal modeling.

Designed to consider spatial interactions, the theory of metapopulations allows the special geographical environment of the Island to be included in the original model. This metapopulation network was created based on real geographical and demographical data. It could then handle local interactions between nodes and thus allow population mobilities to become part of the model too.

We proposed two mobility models. The first one, for humans, is based on the analysis of real human mobility data sets (mobile phone probes). The second model, for mosquitoes, is based on local interactions between nodes.

After various studies of the consequences of mobilities on the spread of the disease, and after an analysis of the parameters of the system, a validation of the model against real seroprevalence data from the Réunion epidemic was proposed. Results validate the approach and clearly identify human mobility as a key parameter in the spread of such an epidemic.

As stated above, the choice in this work was to focus on mobilities. However, other recognized issues play a key role in the all processes. For instance, the effect of rainfall and weather seasons is known to directly influence mosquito evolution stages (especially aquatic phases). Studying the effect of seasons on the epidemic is definitely a perspective of this work.

Finally, the integration of the metapopulation model and mobilities contributed to increase the complexity of the model. This last model which has only been explored on a numerical basis would need an analytical study.

Acknowledgment

The authors would like to thank the InVS and particularly Ms. Elsa Balleydier, epidemiologist at *CIRE Océan Indien, InVS* in Saint Denis, Réunion Island, France, for their help and availability. This work is partially supported by the "Région Haute-Normandie".

Appendix A

Let $V_{i\rightarrow}=\{k\neq i\ :\ g_i m_{ki}>0\}$ and $V_{\rightarrow i}=\{k\neq i\ /\ g_k m_{ik}>0\}$ be sets of nodes that can be accessed *directly* from city i and nodes that have a *direct* travel access to city i, respectively. Let

$$\mathcal{A}_{i\rightarrow}=\{k\neq i/\exists(k_1,\ldots,k_q)\ \text{distincts},\ m_{k_1 i}m_{k_2 k_1}\cdots m_{k k_q}>0 \ \text{and}\ g_i g_{k_1}\cdots g_{k_q}>0\}$$

$$\mathcal{A}_{\rightarrow i}=\{k\neq i/\exists(k_1,\ldots,k_q)\ \text{distincts},\ m_{k_1 k}m_{k_2 k_1}\cdots m_{i k_q}>0 \ \text{and}\ g_k g_{k_1}\cdots g_{k_q}>0\}$$

be sets of nodes that can be accessed from city i and nodes that have an access to city i, respectively.

Proof of Theorem 3.4. Assume that node 1 is at the DFE (without loss of generality), *i.e.* $I_{Hk1}=0,\ \forall k=1,\ldots,n$ and $I_{m1}=0$. From Eq. (3c), we have $dI_{H11}/dt=\sum_{k=1}^{n} r_{1k}I_{H1k}$. But node $i=1$ is at the DFE, *i.e.* $dI_{H11}/dt=0$, and since $r_{1\nu}>0,\ \forall\nu\in V_{1\rightarrow}$, then, $I_{H1\nu}=0$, $\forall\nu\in V_{1\rightarrow}$. Consider now Eq. (3d) with $i=1$ and let $\nu\in V_{1\rightarrow}$, then

$$\frac{dI_{H1\nu}}{dt}=\beta_{H\nu}\frac{I_{m\nu}}{N_{H\nu}^{p}}S_{H1\nu}$$

As system (3) is at an equilibrium point, thus $dI_{H1\nu}/dt=0$. However, $\beta_{H1}>0$ and $S_{H1\nu}>0$ from Proposition 3.1, then $Im_\nu=0$ for all $\nu\in V_{1\rightarrow}$. Finally, we have to show that for all $\nu\in V_{1\rightarrow}$ and for all $k=1,\ldots,n$, $I_{Hk\nu}=0$ *i.e.*, all humans residents of node k and present at node ν are not infected. Consider Eq. (3f) for a node $\nu\in V_{1\rightarrow}$, then

$$\begin{aligned}\frac{dI_{m\nu}}{dt}&=\sum_{j=1}^{n}\beta_{m\nu}\frac{S_{m\nu}I_{Hj\nu}}{N_{H_i}^{p}}-d_m I_{m\nu}=\beta_{m\nu}\frac{S_{m\nu}}{N_{H_i}^{p}}\sum_{j=1}^{n}I_{Hj\nu}\\&=\beta_{m\nu}\frac{S_{m\nu}}{N_{H\nu}^{p}}I_{H\nu}^{p}=0\end{aligned}$$

Since $\beta_{m\nu}>0$, and from Proposition 3.1, $S_{m\nu}>0$ then $I_{H\nu}^{p}=0$, *i.e.* $\sum_{k=1}^{n}I_{Hk\nu}=0$. It follows that for all $k=1,\ldots,n$, $I_{Hk\nu}=0$, since $I_{Hij}\geq 0$ for all $i,j=1,\ldots,n$. Thus, all adjacent nodes to node $i=1$ are the DFE equilibrium. Moreover, by induction, we obtain that all nodes $\nu\in\mathcal{A}_{1\rightarrow}$ are at the DFE.

Assume now that M^T is irreducible. From Eq. (3d) with $j=1$, we have $dI_{Hi1}/dt=g_i m_{1i}I_{Hii}$. Since the system is at equilibrium $dI_{Hi1}/dt=0$, besides $g_i m_{1i}>0$ for $i\in\mathcal{V}_{\rightarrow 1}$, then $I_{Hii}=0$ for all $i\in\mathcal{V}_{\rightarrow 1}$. Let $\nu\in\mathcal{V}_{\rightarrow 1}$, from Eq. (3c), we have

$$\frac{dI_{H\nu\nu}}{dt}=\sum_{k=1}^{n}r_{\nu k}I_{H\nu k}+\beta_{Hi}\frac{I_{m\nu}}{N_{H\nu}^{p}}S_{H\nu\nu}=0$$

then $\sum_{k=1}^{n}r_{\nu k}I_{H\nu k}=0$ and

$$\beta_{Hi}\frac{I_{m\nu}}{N_{H\nu}^{p}}S_{H\nu\nu}=0$$

and $S_{H\nu\nu}>0$, from Proposition 3.1, thus $I_{m\nu}=0$ for all $\nu\in\mathcal{V}_{\rightarrow 1}$. Finally, consider Eq. (3f) for $\nu\in\mathcal{V}_{\rightarrow 1}$, we have

$$\frac{dI_{m\nu}}{dt}=\beta_{m\nu}\frac{S_{m\nu}}{N_{H\nu}^{p}}I_{H\nu}^{p}=0$$

then $I_{H\nu}^{p}=0$, *i.e.* $\sum_{k=1}^{n}I_{Hk\nu}=0\ \forall k=1,\ldots,n$. Thus all nodes are at the DFE. □

Proof of Theorem 3.6. Assume that the disease is endemic in node $i=1$, *i.e.* there exists $q\in 1,\ldots,n$ such that $I_{Hq1}>0$. We have to show that, in this case, $I_{H11}>0$. If $q=1$ then we can proceed. Assume that $q\neq 1$. Assume by contradiction that $I_{H11}=0$.

Since the system is at equilibrium, from (3c), we have

$$0 = \frac{dI_{H11}}{dt} = + \sum_{k=1}^{n} r_{1k} I_{H1k} + \beta_{H1} \frac{I_{m1}}{N_{H_1}^p} S_{H11}$$

Besides $\beta_{Hi} > 0$ and $S_{H11} > 0$ then $I_{m1} = 0$. Thus, from Eq. (3f), we have

$$0 = \frac{dI_{m1}}{dt} = \sum_{j=1}^{n} \beta_{mi} \frac{I_{Hj1}}{N_{H_i}^p} S_{m1}$$

Besides $\beta_{mi} > 0$ and $S_{mi} >$ then $I_{Hj1} = 0$ for all $j = 1, \ldots n$, which is a contradiction. We have $I_{H11} > 0$, if the disease is endemic in node 1, which we now assume.

Consider Eq. (3d) with $i = 1$ and $j \neq i$. Assume $I_{Hij} = 0$. Since the system is at equilibrium, we have

$$0 = \frac{dI_{Hij}}{dt} = g_1 m_{j1} I_{H11} + \beta_{Hj} \frac{I m_j}{N_{H_j}^p} S_{Hij}$$

If $j \in \mathcal{V}_{1\rightarrow}$ then $g_1 m_{j1} > 0$ thus $I_{Hii} = 0$, which is a contradiction. Finally $I_{H1j} > 0$ for all $j \in \mathcal{V}_{1\rightarrow}$, which means that the disease is endemic. Particularly, we deduce that $I_{Hjj} > 0$ from the first part of the proof. By continuing, we can show that the disease is endemic in all nodes $j \in \mathcal{A}_{1\rightarrow}$, that is to say, nodes reachable from node 1. □

References

Arino, J., 2009. Diseases in metapopulations. In: Ma, Z., Zhou, Y., Wu, J. (Eds.), Modeling and Dynamics of Infectious Diseases. Series in Contemporary Applied Mathematics, vol. 11. World Scientific, pp. 65–123.

Arino, J., van den Driessche, P., 2003. A multi-city epidemic model. Math. Popul. Stud. 10, 175–193.

Arino, J., Davis, J., Hartley, D., Jordan, R., Miller, J., van den Driessche, J., 2005. A multi-species epidemic model with spatial dynamics. Math. Med. Biol. 22 (June (2)), 129–142.

Auger, P., Kouokam, E., Sallet, G., Tchuente, M., Tsanou, B., 2008. The ross-macdonald model in a patchy environment. Math. Biosci. 216 (2), 123–131.

Bacaër, N., 2007. Approximation of the basic reproduction number r0 for Vector-Borne diseases with a periodic vector population. Bull. Math. Biol. 69 (3), 1067–1091.

Bailey, N.T.J., 1980. Spatial models in the epidemiology of infectious diseases. in: Biological Growth and Spread (Proceedings of the Conference, Heidelberg, 1979). Lecture Notes in Biomath., vol. 38. Springer, Berlin, pp. 233–261.

Balcan, D., Gonçalves, B., Hu, H., Ramasco, J.J., Colizza, V., Vespignani, V., 2010. Modeling the spatial spread of infectious diseases: the global epidemic and mobility computational model. J. Computat. Sci. 1 (3), 132–145.

Colizza, V., Vespignani, A., 2008. Epidemic modeling in metapopulation systems with heterogeneous coupling pattern: theory and simulations. J. Theoret. Biol. 251 (3), 450–467.

Cosner, C., Beier, J., Cantrell, R., Impoinvil, D., Kapitanski, L., Potts, M., Troyo, A., Ruan, S., 2009. The effects of human movement on the persistence of vector-borne diseases. J. Theoret. Biol. 258 (4), 550–560.

Cui, J., Takeuchi, Y., Saito, Y., 2006. Spreading disease with transport-related infection. J. Theoret. Biol. 239 (3), 376–390.

Delatte, H., Gimonneau, G., Triboire, A., Fontenille, D., 2009. Influence of temperature on immature development, survival, longevity, fecundity, and gonotrophic cycles of aedes albopictus, vector of chikungunya and dengue in the Indian Ocean. J. Med. Entomol. 46, 33–41.

Dumont, Y., Chiroleu, F., 2010. Vector control for the chikungunya disease. Math. Biosci. Eng. 7 (2), 313–345.

Dushoff, X., Levin, S., 1995. The effects of population heterogeneity on disease invasion. Math. Biosci. 128 (1–2), 25–40.

Fitzgibbon, W.E., Langlais, M., 2003. A diffusive SIS model describing the propagation of FIV. Commun. Appl. Anal. 7 (2–3), 387–403.

González, M.C., Hidalgo, C.A., Barabási, A., 2008. Understanding individual human mobility patterns. Nature 453 (7196), 779–782.

Gratz, N.G., 1999. Emerging and resurging vector-borne diseases. Ann. Rev. Entomol. 44 (1), 51–75.

Hackett, L.W., 1958. The epidemiology and control of malaria. Am. J. Trop. Med. Hyg. 7 (5), 577–578.

INSEE *Estimations carroyées de population en 2007*, ⟨http://www.insee.fr/fr/ppp/bases-de-donnees/donnees-detaillees/duicq/regionasp?reg=04⟩ (02 2012).

Knobler, S., Mahmoud, A., Lemon, S., Pray, L., 2006. The Impact of Globalization on Infectious Disease Emergence and Control: Exploring the Consequences and Opportunities, Workshop Summary—Forum on Microbial Threats, The National Academies Press.

Levins, R., 1969. Some demographic and genetic consequences of environmental heterogeneity for biological control. Bull. Entomol. Soc. Am. 5555 (15), 237–240.

Lloyd, A.L., May, R.M., 1996. Spatial heterogeneity in epidemic models. J. Theoret. Biol. 179 (1), 1–11.

Longini Jr., I.M., 1988. A mathematical model for predicting the geographic spread of new infectious agents. Math. Biosci. 90 (1-2), 367–383.

Martens, P., Hall, L., 2000. Malaria on the move: human population movement and malaria transmission. Emerg. Infect. Dis. 6 (2), 103–109.

Menach, A., McKenzie, F.E., Flahault, A., Smith, D., 2005. The unexpected importance of mosquito oviposition behaviour for malaria: non-productive larval habitats can be sources for malaria transmission. Malaria J. 4 (1), 23.

Moulay, D., Aziz-Alaoui, M., Cadivel, M., 2011. The chikungunya disease: modeling, vector and transmission global dynamics. Math. Biosci. 229 (1), 50–63.

Moulay, D., Aziz-Alaoui, M., Kwon, H., 2012. Optimal control of chikungunya disease: larvae reduction, treatment and prevention. Math. Biosci. Eng. 9 (2), 369–392.

Murray, J., 2002. Mathematical Biology II: Spatial Models and Biomedical Applications, 3rd ed. Springer-Verlag.

Nishida, G., Tenorio, J., 1993. What Bit Me? Identifying Hawaii's Stinging and Biting Insects and Their Kin. University of Hawaii Press.

Openstreetmap ⟨http://www.openstreetmap.org/⟩ (02 2012).

Ross, R., 1910. The Prevention of Malaria by Ronald Ross. Murray.

Rvachev, L.A., Longini Jr., I.M., 1985. A mathematical model for the global spread of influenza. Math. Biosci. 75 (1), 3–22.

Sattenspiel, L., Simon, C.P., 1988. The spread and persistence of infectious diseases in structured populations. Math. Biosci. 90 (1–2), 341–366.

Smith, D.L., Dushoff, J., McKenzie, F.E., 2004. The risk of a mosquito-borne infection in a heterogeneous environment. PLoS Biol. 2 (11), e368.

Sutherst, R.W., 2004. Global change and human vulnerability to vector-borne diseases. Clin. Microbiol. Rev. 17 (1), 136–173.

Tsanou, B., 2011. Etude de quelques modèles epidémiologiques de métapopulations: Application au paludisme et à la tuberculose. Ph.D. Thesis. University Paul Verlaine of Metz and University of Yaoundé, 2011.

Vazeille, M., Moutailler, S., Coudrier, D., Rousseaux, C., Khun, H., Huerre, M., Thiria, J., Dehecq, J.-S., Fontenille, D., Schuffenecker, I., Despres, P., Failloux, A.-B., 2007. Two chikungunya isolates from the outbreak of la reunion (Indian Ocean) exhibit different patterns of infection in the mosquito, aedes albopictus. PLoS ONE 2 (11), e1168.

Vermillard, G., 2009. Le chikungunya: un virus, une maladie - a propos de l'épidémie 2005-2006 à l'ile de la réunion. Ph.D. Thesis. UHP—Université Henri Poincaré.

Wang, W., Zhao, X.-Q., 2004. An epidemic model in a patchy environment. Math. Biosci. 190 (1), 97–112.

Zongo, P., 2008. Modélisation mathématique de la dynamique de transmission du paludisme, Ph.D. Thesis.